Chinese Journal of Chemical Engineering 85 (2025) 66–75

Contents lists available at ScienceDirect

Chinese Journal of Chemical Engineering

journal homepage: www.elsevier.com/locate/CJChE

Full Length Article

Study on the desalination efficiency of hydrate phase by a pressure-driven filtration method

Yiwei Wu [#], Zhenbin Xu [#], Xiaohui Wang [*], Jin Cai , Tenghua Zhang , Peng Xiao , Changyu Sun , Guangjin Chen

State Key Laboratory of Heavy Oil Processing, China University of Petroleum, Beijing 102249, China

ARTICLE INFO

Article history:
Received 17 December 2024
Received in revised form
17 March 2025
Accepted 18 March 2025
Available online 12 April 2025

Keywords:
Desalination
Gas hydrate
Pressure-driven filtration
Salt removal efficiency
Multi-stage

ABSTRACT

The mechanism of hydrate-based desalination is that water molecules would transfer to the hydrate phase during gas hydrate formation process, while the salt ions would be conversely concentrated in the unreacted saltwater. However, the salt concentration of hydrate decomposed water and the desalination degree of hydrate phase are still unclear. The biggest challenge is how to effectively separate the hydrate phase and the remaining unreacted salt water, and then decompose the hydrate phase to measure the salt concentration of hydrate melt water. This work developed an apparatus and pressure-driven filtration method to efficiently separate the hydrate phase and the remaining unreacted saltwater. On this basis, the single hydrate phase was obtained, then it was dissociated and the salt concentration of hydrate melt water was measured. The experimental results demonstrate that when the initial salt mass concentration is 0.3% to 8.0%, the salt removal efficiency for NaCl solution is 15.9% to 29.8% by forming CO_2 hydrate, while for $CaCl_2$ solution is 28.9% to 45.5%. The solute $CaCl_2$ is easier to be removed than solute NaCl. In addition, the salt removal efficiency for forming CO_2 hydrate is higher than that for forming methane hydrate. The multi-stage desalination can continuously decrease the salt concentration of hydrate dissociated water, and the salt removal efficiency per stage is around 20%.

1. Introduction

Freshwater is valuable resource for the survival of the human beings and the entire ecosystem [1–3]. However, the freshwater resources only account for 2.5% of the Earth's water resources, and their distribution is uneven, which cannot guarantee people's daily water use [4,5]. Therefore, seawater desalination technology is of great importance for the human beings [6,7]. Currently, common seawater desalination technologies include solar assisted evaporation [8–10], membrane separation [11–13], electrochemical treatment [14–16] and reverse osmosis [17,18], *etc.*

A new type of seawater desalination method based on hydrate technology has received widespread attention due to its advantages of low energy consumption, simple equipment, and environmental protection [19–22]. Hydrate seawater desalination technology utilizes the salt removal effect of the hydrate formation process. At the end of hydrate formation process, the solid hydrate phase is separated from the remaining unreacted water, and decomposes the hydrate to obtain fresh water. Parker [23] firstly proposed the concept of seawater desalination based on the hydrate method. Dickens and Quinby-Hunt [24] determined the phase equilibrium conditions of methane hydrate in seawater. The results show that compared with pure water system, the average decomposition temperature of methane hydrate in seawater system decreases by about 1.1 K. Due to the unique cage-like structure of gas hydrate formed at lower temperature and higher pressure [25,26], water molecules will transfer to the hydrate phase, while the salt will concentrate in the unreacted saline water [27,28]. Sun *et al.* [29] evaluated the potential of the Span 80 enhanced HBD technology to treat highly concentrated brine solutions, heavy metal wastewater, and strongly acidic or alkaline solutions, as well as the performance of a multi-stage desalination process. Ling *et al.* [30] used a graphite-promoted single-stage desalination method to test the desalination and Li enrichment properties during the formation process of cyclopentane (CP) hydrate. Mi *et al.* [31] studied the effect of different C_3H_8 concentration on the formation of CO_2/

* Corresponding author.
E-mail address: xh.wang@cup.edu.cn (X. Wang).
# These authors contributed equally to this work.

https://doi.org/10.1016/j.cjche.2025.03.010

C_3H_8 mixed hydrates in brine, which is helpful for the development of hydrate-based desalination technology. Abulkhair *et al.* [32] carried out a single-stage desalination experiment based on CO_2+C_3H_8 hydrate. Mok *et al.* [33] theoretically studied the maximum water production rate and efficiency, the optimization temperature of desalination by forming cyclopentane hydrate, providing important guidance for process operators to choose the optimal operating conditions of hydrate-based desalination (HBD) from a thermodynamic perspective. Maniavi Falahieh *et al.* [34] proposed a mixed seawater desalination method based on CO_2 hydrate, which can remove approximately 82% Na^+ and 100% K^+, Ca^{2+} and Mg^{2+}. Salilih *et al.* [35] conducted thermal analysis on integrated hydrate seawater desalination system and intermediate fluid liquefied natural gas vaporizers, and conducted thermal analysis on the proposed hydrate desalination system. The above researches have proved the feasibility of hydrate-based seawater desalination, and focusing on the industrial scale experiments.

At the end of the hydrate formation stage, the system usually consists of gas phase, hydrate phase and remaining unreacted liquid phase. The first challenge faced by HBD is how efficiently separate the solid hydrate phase and the residual unreacted concentrated saltwater, so as to dissociate hydrate phase to gain fresh water. This step would significantly determine the desalination efficiency and the industrial feasibility of HBD [30]. Zheng and Yang [1] used gas to blow the surface of hydrate phase at low temperature, and the average desalination efficiency after gas blowing is about 75%. Abulkair *et al.* [19] designed a filter at the bottom of the reactor to separate the hydrate from the residual brine. Lv *et al.* [25] used deionized water to wash the hydrate crystals so as to flush away the residual brine, which significantly improves the desalination efficiency. Fakharian *et al.* [28] designed a reactor with separation container that can continuously separate hydrate from water and gas. Park *et al.* [36,37] designed a plant for the continuous production and granulation of CO_2 hydrate through the extrusion operation of a two-cylinder unit. Chen *et al.* [38] used freeze-thaw combined with liquid rinsing, and the final sodium chloride removal efficiency ranged from 29.0% to 64.3%. Montazeri *et al.* [39] used vacuum filtration to separate gas hydrate and residual saline water. Truong-Lam *et al.* [40] designed a new device that can be divided into hydrate formation zone and hydrate compression zone. In the hydrate formation zone, the device combines a plastic scraper with a stirring device, and hydrate crystals are easily aggregated and attached to the reactor wall after formation. Then the stirring device rotates, driving the scraper to scrape off the hydrate crystals on the inner wall and collecting them in the hydrate extrusion zone. The hydrate extrusion zone is a double piston unit structure that can separate the collected hydrates and residual salt water again. Babu *et al.* [41] designed a cylindrical annular bed reactor, and the inner wall is composed of a metal mesh. Hydrates were generated on the surface of the metal mesh, and then the hydrate crystals attached to the metal mesh were scraped off by rotating the scraper on the agitator. The remaining saline water was discharged from the bottom. Han *et al.* [42] further pointed out that the phenomenon of surface adhesion of hydrate crystals and salt entrainment in the gaps between crystals is the main obstacle to the commercial application of HBD separation technology. Therefore, they used three techniques, namely centrifugal separation, water washing, and sweating, to further study the desalination treatment of cyclopentane hydrate crystals. They found that the centrifugal separation has the highest desalination efficiency, about 96%, but the cost is the highest, indicating that the water washing method may have more application prospects. However, the water washing method is anti-mixing behavior for desalination process that would seriously reduce the dehydration efficiency and practical feasibility of the technology. Therefore, how to simply and effectively separate hydrate phase from the remaining unreacted saltwater is a tricky problem.

The objective of this work is to develop a pressure-driven filtration method that is easy to operate and can efficiently separate the solid hydrate phase and remaining unreacted saltwater to the most extent. Based on this method, the performance of the seawater desalination by hydrate method was studied. The desalination efficiency of different kinds of salt solution and different guest gas species were studied. In addition, the amount of formed hydrate, water conversion rate and multi-stage separation were also investigated.

2. Experimental

2.1. Experimental materials and equipment

The sodium chloride (NaCl, ≥99.5%) and calcium chloride ($CaCl_2$, ≥99.5%) were purchased from Xilong Chemical Co., Ltd. (China). CH_4 and CO_2 with purity of 99.9% were purchased from Beijing Haipu Beifen Gas Industry Co., Ltd. (China). The deionized (DI) water ($<10^{-4}$ S·m^{-1}) used to prepare the seawater was purchased from Beijing Hengwei Xingye Scientific Instrument Co., Ltd. (China).

The schematic diagram of single-stage seawater desalination experimental apparatus is shown in Fig. 1. It consists of a sapphire reactor, a gas storage tank, and a data acquisition system (DAS), which has been introduced in previous works [43,44]. The platinum resistance temperature sensor was installed at the top of the sapphire reactor. The pressure sensors were installed at the top and bottom of sapphire reactor, respectively. A piston was installed inside the sapphire reactor and can be controlled by a hand pump. In order to improve gas–liquid mass transfer, a magnetic stirrer was installed in the reactor. A metal sinter-plate filter was installed at the bottom of the sapphire reactor, which can achieve the separation of solid hydrate crystals and unreacted salt water. The temperature of the entire system is controlled by an air bath. Monitor and control generated system (MCGS) can record experimental temperature and pressure per minute.

The schematic diagram of multi-stage seawater desalination experimental apparatus is shown in Fig. 2. It consists of a vertical tubular high-pressure vessel (2500 mm × 38 mm) and auxiliary equipments. The bottom of the high-pressure vessel is made of PEEK material, through which the formation and decomposition of gas hydrate can be visually observed. The maximum working pressure of the high-pressure vessel is 15 MPa. The piston was installed inside the high-pressure vessel and connected to the hand pump. The auxiliary equipment consists of a water bath (273.15–373.15 K), a gas cylinder and a data acquisition system. The accuracies of platinum resistance thermometer detector (Pt 100) and a pressure sensor are 0.1 K and 0.01 MPa, respectively. Similarly, a metal sinter-plate filter was installed at the bottom to separate solid hydrate crystals and the discharged brine.

2.2. Experimental procedures

(1) Establishing the standard curve

In order to determine the salt concentration of hydrate dissociated water, it has to establish the standard curve firstly. The multiple concentrations of NaCl and $CaCl_2$ standard solution were firstly prepared, then the conductivity of each standard solution was measured. The experimental results are shown in Fig. 3. The conductivity meter (FiveEasy Plus FE38) was purchased from Mettler Toledo Instruments Co., Ltd. (Switzerland), with a range of 0.01–500 mS·cm^{-1} and an accuracy of ±0.5% F.S.

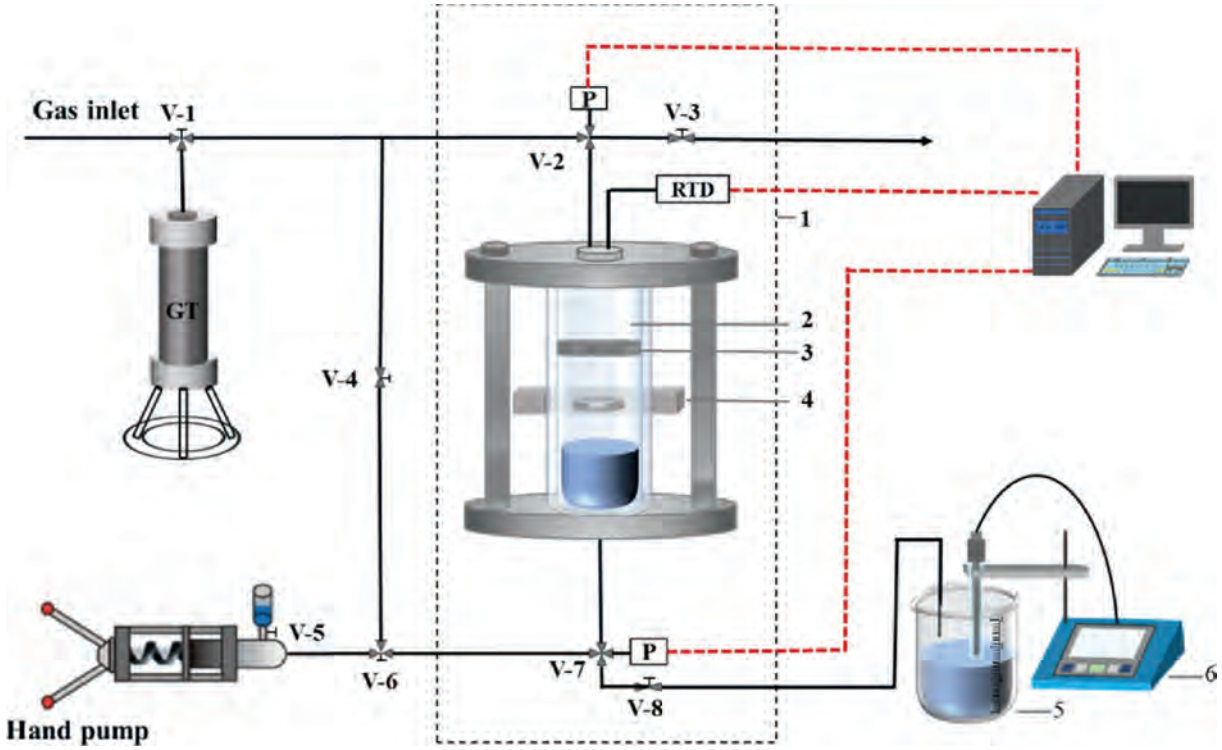

Fig. 1. The schematic diagram of a single-stage seawater desalination apparatus: 1 – air bath; 2 – sapphire cell; 3 – piston; 4 – magnetic stirrer; 5 – beaker; 6– conductivity meter; V – 1,2,3,4,5,6,7,8 – valves; GT – gas tank; RTD – Pt resistance temperature detector; P – pressure transducer.

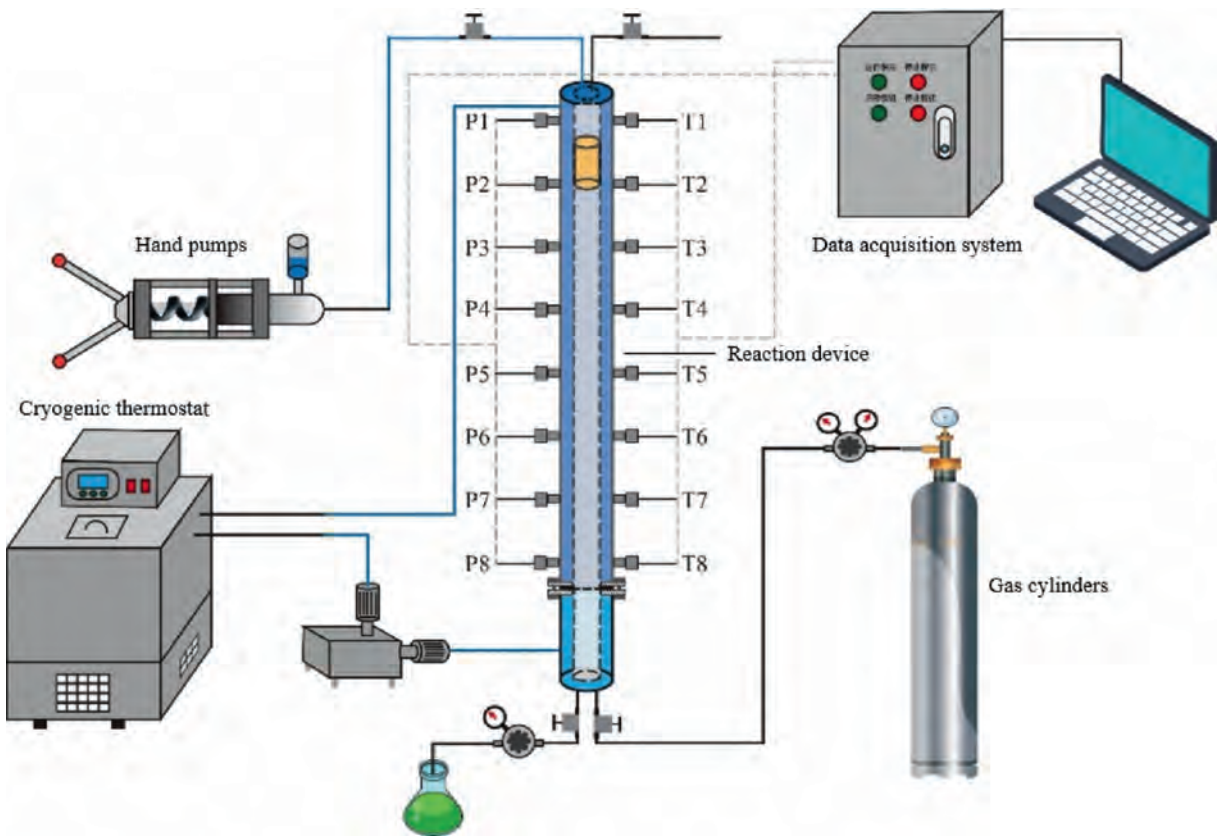

Fig. 2. Schematic diagram of multi-stage seawater desalination experimental apparatus.

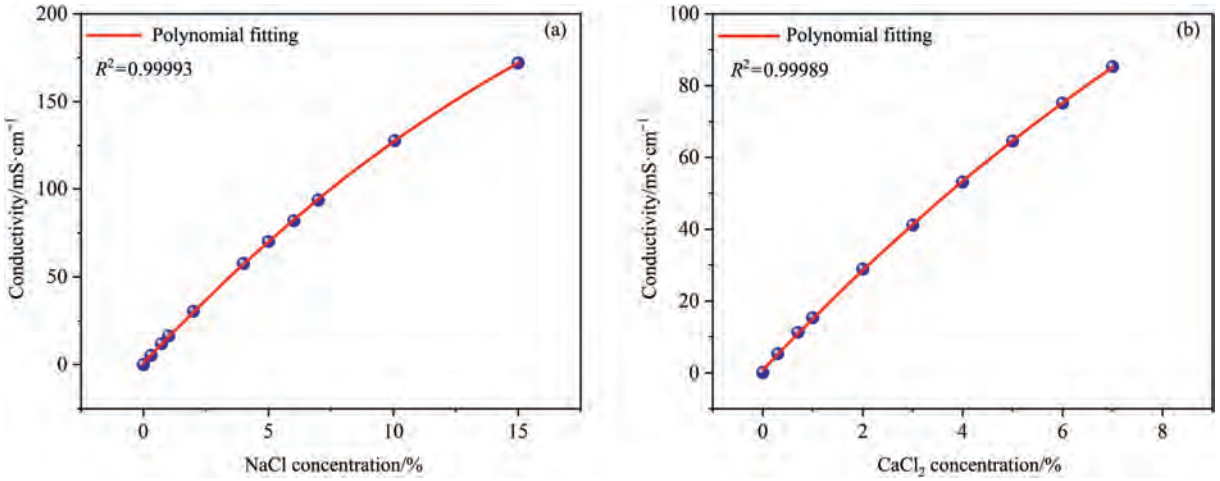

Fig. 3. The relationship between conductivity and salt mass concentration for (a) NaCl solution and (b) $CaCl_2$ solution.

Based on the experimental data, the standard curves between the salt concentration and conductivity of NaCl and $CaCl_2$ solution are achieved by polynomial fitting, as shown in Eqs. (1) and (2).

$$\sigma_1 = -0.243c_s^2 + 15.038c_s + 0.837 \quad (1)$$

$$\sigma_2 = -0.365c_s^2 + 14.603c_s + 0.741 \quad (2)$$

where c_s represents the mass fraction of salt. σ_1 represents the conductivity of NaCl solution, mS·cm^{-1}. σ_2 represents the conductivity of $CaCl_2$ solution, mS·cm^{-1}.

(2) Experimental procedures

The NaCl or $CaCl_2$ was firstly dissolved into the deionized water to prepare salt solution with predicted concentration. The initial conductivity of prepared salt solution was measured by conductivity meter. The reactor and pipelines were cleaned twice with the prepared salt solution. Then the air bath was turned on and the experimental temperature was set at the 274.15 K. 30 ml saltwater was injected into the reactor through a hand pump. The gas was added into the reactor until reaching the experimental pressure. The magnetic stirrer was turned on to accelerate hydrate formation process. During the experiment, the system pressure inside the reactor can be controlled by adjusting the position of piston. When a large amount of gas hydrate has formed, the growth rate of gas hydrate would become extremely slow and the curve of system pressure tends to stabilize. The hydrate sample preparation stage can be end.

After that, the solid hydrate crystals and remaining unreacted saltwater and gas were separated by pressure-driven filtration method through moving the position of internal piston. The schematic diagram and actual pictures of the experimental procedures are shown in Figs. 4 and 5, respectively. Firstly, the concentrated saline water was discharged from the outlet. The conductivity of the unreacted saline water was measured by the conductivity meter. Secondly, the piston kept moving downward to discharge the gas phase and tightly compress the gas hydrate. Thirdly, the piston was moved upward, gas hydrate would begin to decompose under depressurization. After the gas hydrate has been totally decomposed, the hydrate melt water was collected, and the conductivity of the corresponding melt water was measured and used to determine the salt concentration.

(3) Calculation equations

The difference between the initial salt concentration of fresh brine and the salt concentration of hydrate melt water *versus* the initial salt concentration of fresh brine is defined as the desalination efficiency factor (η_d), as shown in Eq. (3).

$$\eta_d = \frac{c_0 - c_1}{c_0} \times 100\% \quad (3)$$

where c_0 and c_1 represent the mass fractions of salt in the initial fresh brine and the hydrate dissociated water, respectively.

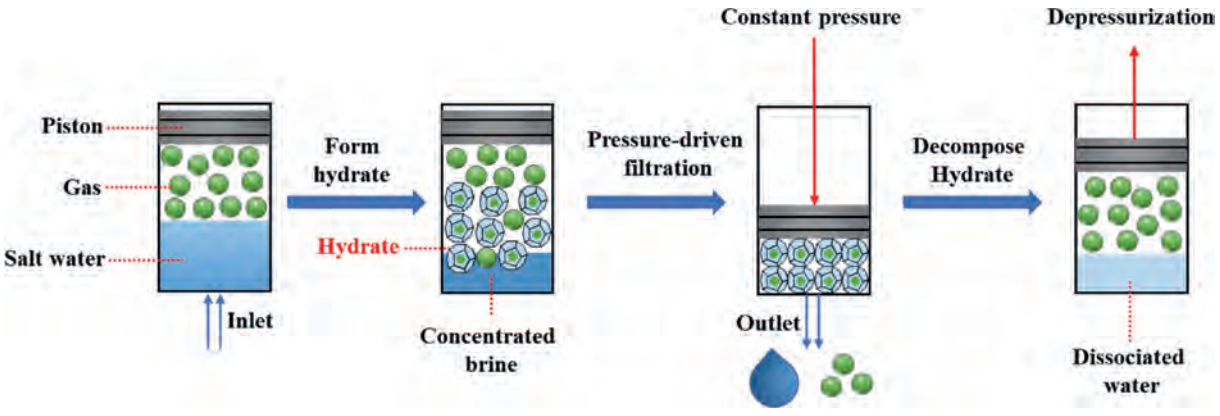

Fig. 4. Schematic diagram of pressure-driven filtration method for studying the seawater desalination by HBD.

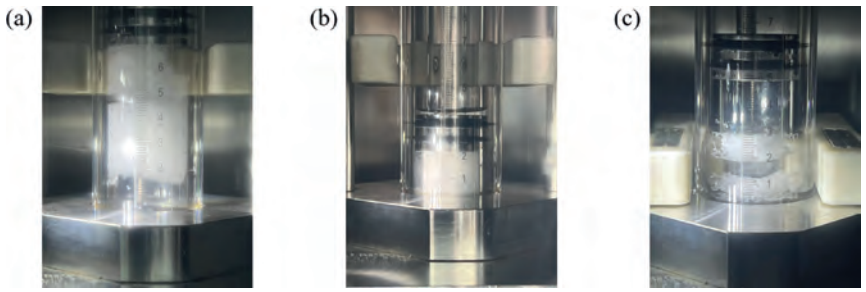

Fig. 5. The actual pictures taken during the experiment: (a) preparing hydrate sample, (b) discharge the residual unreacted brine and gas, accompanying by tightly compress solid hydrate crystals, (c) the piston was moved upward to decompose gas hydrate. The experimental conditions are summarized in Table 1. *P* and *T* represent the experimental pressure and temperature during hydrate formation process, respectively.

Table 1
The experimental conditions of HBD.

Run No.	Guest molecule	Salt type	Salt mass concentration/ %	Compaction pressure/ MPa	*P*/MPa	*T*/K	Desalination stage
1-1	CO_2	NaCl	3.5	3.0	3.5	274.15	Single
1-2	CO_2	NaCl	3.5	3.5	3.5	274.15	Single
1-3	CO_2	NaCl	3.5	4.0	3.5	274.15	Single
1-4	CO_2	NaCl	3.5	5.0	3.5	274.15	Single
1-5	CO_2	NaCl	3.5	6.0	3.5	274.15	Single
1-6	CO_2	NaCl	3.5	7.0	3.5	274.15	Single
1-7	CO_2	NaCl	3.5	8.0	3.5	274.15	Single
2-1	CO_2	NaCl	0.3	5.0	3.5	274.15	Single
2-2	CO_2	NaCl	1.0	5.0	3.5	274.15	Single
2-3	CO_2	NaCl	2.0	5.0	3.5	274.15	Single
2-4	CO_2	NaCl	3.0	5.0	3.5	274.15	Single
2-5	CO_2	NaCl	4.0	5.0	3.5	274.15	Single
2-6	CO_2	NaCl	5.0	5.0	3.5	274.15	Single
2-7	CO_2	NaCl	6.0	5.0	3.5	274.15	Single
2-8	CO_2	NaCl	7.0	5.0	3.5	274.15	Single
2-9	CO_2	NaCl	8.0	5.0	3.5	274.15	Single
3-1	CO_2	$CaCl_2$	0.3	5.0	3.5	274.15	Single
3-2	CO_2	$CaCl_2$	1.0	5.0	3.5	274.15	Single
3-3	CO_2	$CaCl_2$	2.0	5.0	3.5	274.15	Single
3-4	CO_2	$CaCl_2$	3.0	5.0	3.5	274.15	Single
3-5	CO_2	$CaCl_2$	4.0	5.0	3.5	274.15	Single
3-6	CO_2	$CaCl_2$	5.0	5.0	3.5	274.15	Single
3-7	CO_2	$CaCl_2$	6.0	5.0	3.5	274.15	Single
3-8	CO_2	$CaCl_2$	7.0	5.0	3.5	274.15	Single
4-1	CH_4	NaCl	0.3	5.0	10.0	274.15	Single
4-2	CH_4	NaCl	1.0	5.0	10.0	274.15	Single
4-3	CH_4	NaCl	2.0	5.0	10.0	274.15	Single
4-4	CH_4	NaCl	3.0	5.0	10.0	274.15	Single
4-5	CH_4	NaCl	4.0	5.0	10.0	274.15	Single
4-6	CH_4	NaCl	5.0	5.0	10.0	274.15	Single
4-7	CH_4	NaCl	6.0	5.0	10.0	274.15	Single
5-1	CO_2	NaCl	3.5	5.0	3.5	274.15	Three
5-2	CO_2	NaCl	2.0	5.0	3.5	274.15	Three

The water recovery rate of HBD method is defined as Eq. (4).

$$R = \frac{m_1 \times (1 - c_1)}{m_0 \times (1 - c_0)} \times 100\% \quad (4)$$

where m_0 represents the initial mass of brine, g. m_1 represents the mass of the solution decomposed from gas hydrate, g. According to Eq. (4), the water conversion rate for forming gas hydrate is equal to the water recovery rate.

3. Results and Discussion

3.1. The influence of extrusion pressure on desalination efficiency

At the end of the hydrate formation process, the system contains hydrate phase and remaining unreacted gas phase and liquid phase. One of the challenges faced by hydrate-based desalination is how to separate the hydrate phase and the remaining unreacted concentrated saltwater. This work proposes a pressure-driven filtration separation method that can high-efficiently separate hydrate phase and residual unreacted concentrated saltwater. On this basis, the desalination efficiency of HBD was studied.

As for pressure-driven filtration method, the extrusion pressure may significantly affect the separation degree of hydrate phase and liquid phase. Hence, the influence of extrusion pressure on the desalination efficiency was firstly studied. The CO_2 hydrate was formed under 274.15 K and 3.5 MPa, with initial NaCl concentration of 3.5%. According to Fig. 6(a), as the extrusion pressure increases, the desalination efficiency of the hydrate phase would gradually increase. When the extrusion pressure is higher than 5 MPa, the desalination efficiency of the hydrate phase tends to be stable and reach the maximum value. According to Fig. 6(b), the water recovery rate significantly decreases with the increase of extrusion pressure. When the extrusion pressure increases to above 5 MPa, the compaction degree of hydrate crystals tends to stabilize and the water recovery rate tends to stabilize accordingly. It indicates that the solid hydrate has been fully compacted and the residual water was maximally squeezed out. Therefore, the extrusion pressure was set at 5 MPa for subsequent experiments, then the other influence factors, such as water state (salt concentration, types of salt ions, water conversion to the gas hydrate), gas source (guest gas species), and operation mode (single stage, multi-stage) on the desalination efficiency for the hydrate-based desalination method were studied.

3.2. Effect of water conversion rate on desalination efficiency

Owing to the desalination effect of hydrate formation process, the salt concentration in residual liquid phase and in hydrate dissociated water may be affected by the water conversion rate to hydrate phase. Therefore, the water conversion rate is an important parameter in HBD. The NaCl concentration is 3.5%, and the guest gas species is pure CO_2. The water conversion rate was adjusted by controlling the reaction time, and then the residual unreacted liquid phase and gas phases were discharged from the outlet at the bottom of the reactor under the pressure of 5 MPa, accompanied by the filtration and tight compression of hydrate crystals into cylindrical shape. After that, the hydrate crystals were dissociated by depressurization method and the salt concentration of hydrate melt water was measured. According to Fig. 7, the water conversion rate for forming CO_2 hydrate is in the range of 20.39% to 43.01%, and the corresponding desalination efficiency ranges from 52.54% to 20.75%. This result reveals the importance of water conversion rate in desalination efficiency. Although the experimental temperature, pressure, and driving force can be precisely controlled, the quality of the formed hydrate cannot be measured in real-time and

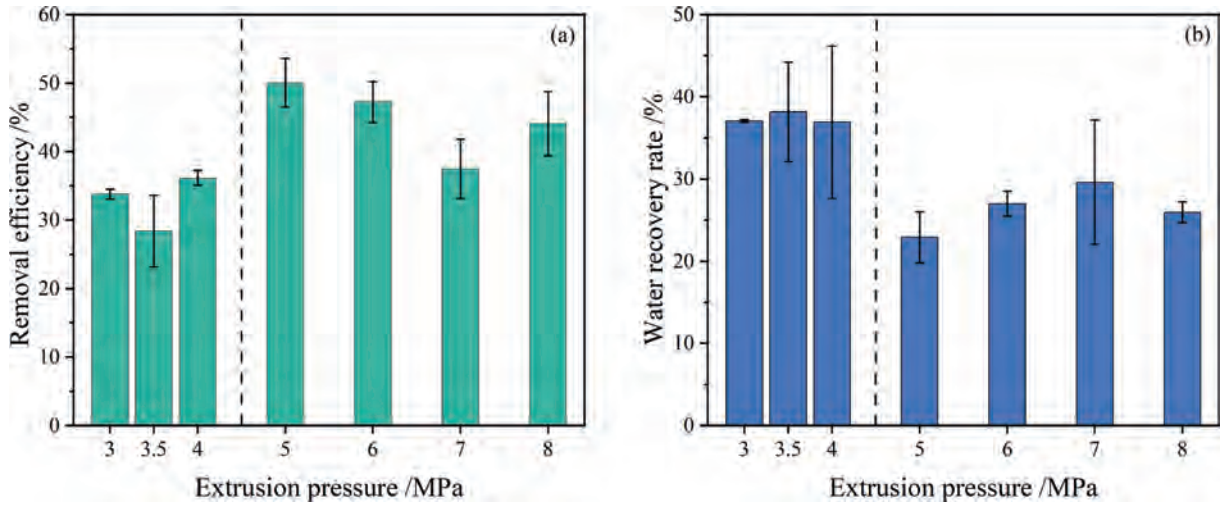

Fig. 6. The relationship between extrusion pressure and desalination efficiency by forming CO_2 hydrate with initial salt concentration of 3.5%: (a) salt removal efficiency, (b) water recovery rate.

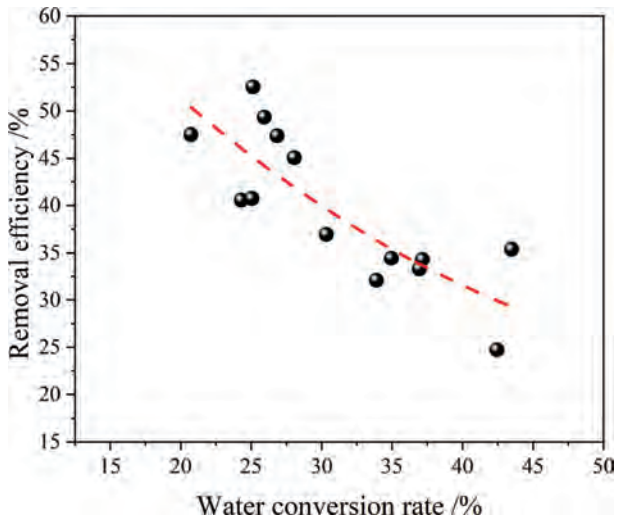

Fig. 7. The relationship between water conversion rate by forming CO_2 hydrate and desalination efficiency at salt concentration of 3.5%.

precisely controlled. Controlling the quality of formed hydrate remains a challenge in experimental research. Therefore, even under the same experimental conditions, the quality of the formed hydrate is not completely the same, resulting in deviations of removal efficiency.

According to Fig. 8, there are many hydrate particles formed during the hydrate formation process. After the drainage stage, there is still some concentrated salt solution remains in the pore space formed by hydrate particles. According to the reported articles [25,42,45], the desalination efficiency can increase to over 80% by applying post-treatment steps, such as DI water washing, centrifuging, and sweating. Therefore, the post-treatment steps can improve the salt removal efficiency by reducing the residual concentrated salt solution in the pore space. The amount of concentrated salt solution remains in the pore space highly depends on the effectiveness of the pressure-driven filtration, which further affect the final desalination efficiency. Previous research works [46,47] show that the surface of gas hydrate is hydrophilic and the hydrate surface is fully wetted by water. Therefore, some concentrated salt solution may also adsorb on the surface of gas

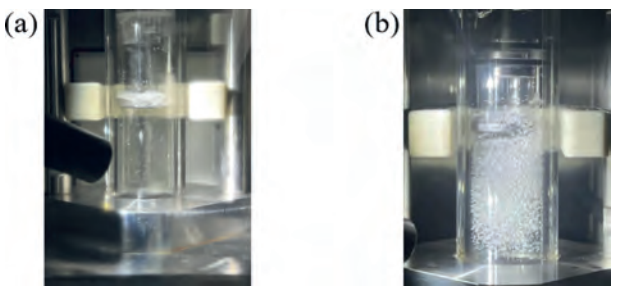

Fig. 8. The picture was taken during the formation of carbon dioxide hydrate in the (a) pure water and (b) NaCl aqueous solution.

hydrate, which is hardly be removed. And this part of salt solution will affect the final desalination efficiency. Therefore, the salt solution remains in the pore space of hydrate particles, and the salt solution adsorbs on the surface of hydrate particles, jointly affecting the final desalination efficiency. According to Fig. 8, compared with hydrate formation in the pure water, the nucleation of CO_2 hydrate in the NaCl solution is widely dispersed in the bulk liquid phase. The presence of NaCl may affect nucleation behavior by changing the local water molecule structure or gas–liquid interface properties [48–51]. It may attach to the surface of hydrate crystals, or mix into the hydrate crystals along with the residual saltwater, even take part in hydrate formation process. This requires further verification through molecular dynamics simulation.

3.3. The influence of salt concentration and ions on the desalination efficiency

Seawater usually contains different kinds of salt ions, such as Na^+, K^+, Ca^{2+}, Mg^{2+}, *etc.* In addition, salt has a significant thermodynamic inhibition effect on the growth of gas hydrate [52,53]. The increase of salt concentration will lead to lower hydrate phase equilibrium temperature and even affect the water conversion ratio to gas hydrate [54–56], which may further affect the desalination efficiency. Therefore, this work investigated the desalination efficiency of seawater with different salt concentration and ion types by HBD. The salt concentration of seawater sample was set from 0.3% to 8.0%, which covers the salt concentration of actual seawater. The desalination efficiency of NaCl and $CaCl_2$ solutions were

studied and compared in this work. When the experimental temperature is 274.15 K, keep increasing pressure may cause CO_2 to transfer from gas phase to the liquid phase. In order to ensure that all experiments were conducted under gaseous CO_2 condition, the salt concentration range of $CaCl_2$ solution is 0.3% to 7.0%, while that of NaCl solution is 0.3% to 8.0%. To compare the desalination efficiency of $CaCl_2$ and NaCl solutions, the horizontal axis was set within the same range, as shown in Fig. 9. The desalination efficiency of NaCl solution by hydrate-based desalination ranges from 15.90% to 29.80%, and has no obviously relationship with salt concentration. Although inorganic salts can change hydrate equilibrium conditions, they wouldn't change hydrate formation rate and even promote hydrate formation rate at low concentration [48–51,57,58]. Meanwhile, all the experimental results show that the desalination efficiencies of $CaCl_2$ solution systems are higher than that of NaCl solution systems. It indicates that solute $CaCl_2$ is easier to be removed than solute NaCl by the HBD. Park *et al.* [36] also found that ion rejection by the hydrate process strongly depends on the ionic size and charge, and the mechanism of ion rejection needs to be clarified. Fig. 7 shows that the desalination efficiency decreases with the increase of water conversion ratio. The more gas hydrates formed, the higher the water conversion ratio, and the corresponding ion concentration in the unreacted residual salt solution will also increase. Solution with higher ion concentrations adsorbs on the surface of gas hydrate, resulting in lower desalination efficiency. On the contrary, solution with lower ion concentration adsorbs onto the surface of gas hydrate, thereby improving desalination efficiency. As shown in Table 2, the water conversion ratio of NaCl solution is higher than that of $CaCl_2$ solution. Therefore, the ion concentration of NaCl solution adsorbed on the surface of gas hydrate is higher than that of $CaCl_2$ solution. This may result in a higher desalination efficiency of HBD for $CaCl_2$ solution than NaCl solution. Therefore, the salt solution adsorbed on the surface of gas hydrate has a significant impact on the desalination efficiency of HBS. Another possibility for the difference in desalination efficiency between NaCl and $CaCl_2$ solutions is that the particle size of CO_2 hydrate crystals may depend on the type of salt present in the system.

3.4. The influence of gas species on the desalination efficiency

The gas species is a key factor for determining the physical properties of gas hydrate. Meanwhile, the guest gas species also can affect hydrate formation conditions, induction time, growth rate, and hydrate crystal structure, which may further affect the desalination efficiency of HBD. Therefore, the gas species is very important for seawater desalination projects. The formation conditions of carbon dioxide hydrates are milder and more suitable for hydrate-based seawater desalination technology [59,60]. However, the offshore oil extraction platform requires a large amount of freshwater resources, which are currently transported by ship. On the other hand, offshore oil extraction platforms have abundant associated gas from oil fields. Therefore, in addition to studying the desalination ability of carbon dioxide hydrate, we also attempted to investigate the potential of hydrate-based desalination by forming alkane hydrate, such as forming methane hydrate. According to Fig. 10(a), when the NaCl concentration is below 3.0%, the desalination efficiency of methane hydrate is higher than that of carbon dioxide hydrate. However, when the initial salt concentration is above 3.0%, the desalination efficiency of methane hydrate becomes lower than that of carbon dioxide hydrate. As shown in Fig. 10(b), when under the same initial salt concentration conditions, the water recovery rate for forming carbon dioxide hydrate is higher than that of forming methane hydrate. On one hand, the hydrate formation conditions of CO_2 hydrate are milder than that of methane hydrate. On the other hand, the experimental results show that for the formation of gas hydrate in the brine, the nucleation of methane hydrate mainly occurs at the liquid–gas surface, while the nucleation of CO_2 hydrate widely dispersed in the bulk liquid phase, as shown in Fig. 8. This may result in that the water conversion for forming CO_2 hydrate is larger than that of forming methane hydrate. Therefore, as for HBD, the CO_2 molecules is better than methane molecules to form gas hydrate, which has higher water recovery rate and salt removal efficiency.

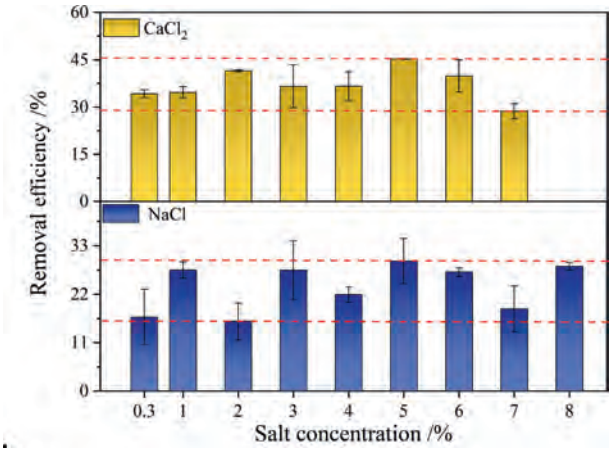

Fig. 9. The relationship between salt mass concentration and the desalination efficiency of CO_2 hydrate.

Table 2
Water conversion ratio in NaCl solution and $CaCl_2$ solution.

Salt mass concentration/%	Water conversion ratio/%	
	NaCl solution	$CaCl_2$ solution
0.3	42.08	36.91
1.0	46.25	30.92
2.0	52.66	31.58
3.0	49.88	37.66
4.0	51.83	36.71
5.0	39.52	29.38
6.0	41.48	28.70
7.0	43.97	36.70
8.0	37.28	–

3.5. Multi-stage seawater desalination efficiency

As discussed in the above experimental results, the desalination efficiency of single stage is mainly below 50% for HBD when the liquid-hydrate two phases were separated by pressure-driven filtration method. In order to further improve the desalination efficiency, it is necessary to continue decreasing the salt concentration of hydrate dissociated water. Therefore, multi-stage operation mode was applied to study the capacity of hydrate-based desalination method. A large-scale experiment setup was designed and developed, as shown in Fig. 2. The experimental procedures of multi-stage hydrate desalination are similar to that of single stage hydrate desalination process. The solid hydrate crystals and concentrated saltwater were separated by pressure-driven filtration method, then followed by hydrate dissociation process. The conductivity of hydrate dissociated water was measured. After that, gas hydrate reformed from the dissociated water and the next recycle process started. The salt removal efficiency of three-stage hydrate desalination experiment was studied in this work. The

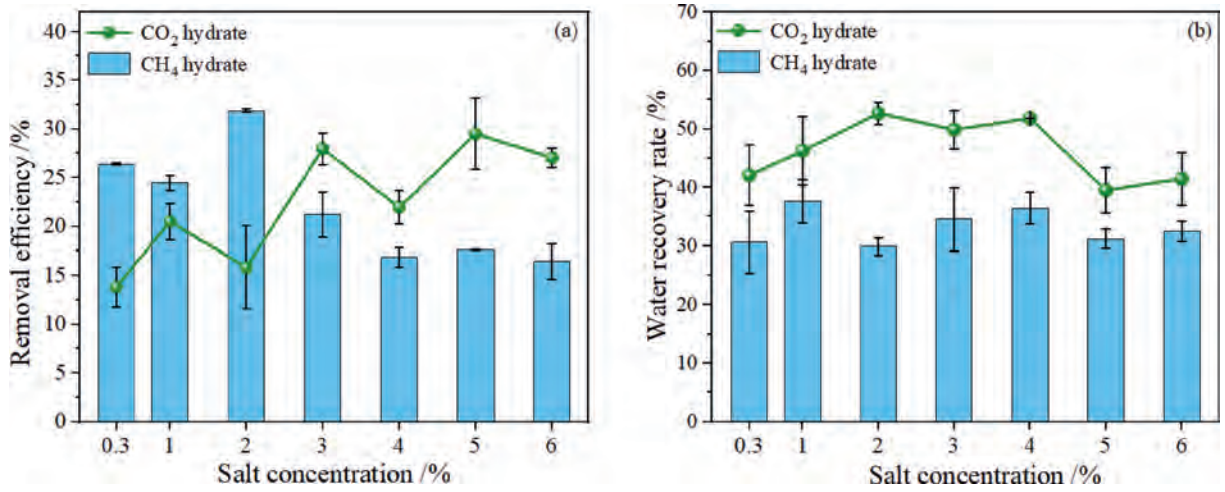

Fig. 10. The relationship between guest types and hydrate desalination efficiency: (a) salt removal efficiency, (b) water recovery rate.

initial NaCl concentration was set at 3.5%, which is close to the actual salt concentration of seawater. The experimental results are shown in Fig. 11. After three stages of seawater desalination experiments, the NaCl concentration decreases from the initial 3.5% to 1.6%, and the cumulative desalination efficiency of the three-stage desalination process was 54.48%. The results indicate that the desalination efficiency at each stage is approximately 23.00%. Therefore, seawater can be desalinated and purified through HBD by adding a seawater desalination stages.

As the salt concentration of hydrate dissociated water after the third stage desalination treatment is still higher than the drinking water standard. Therefore, other three-stages desalination experiment was conducted with initial NaCl concentration of 2.0% to further test the salt concentration of hydrate dissociated water. The experimental results are shown in Fig. 12. After three stages of seawater desalination experiments, the salt concentration decreased from the initial 2.0% to 0.8%. The cumulative desalination efficiency of the three-stage desalination process is 58.76%. The desalination efficiency of each stage is 34.94%, 25.44%, and 14.97%, respectively. The desalination efficiency of each cycle varies, which may be due to different water conversion rate. It proves that HBD is an efficient desalination technology and increasing the desalination stages is a good way to continue to decrease the salt concentration

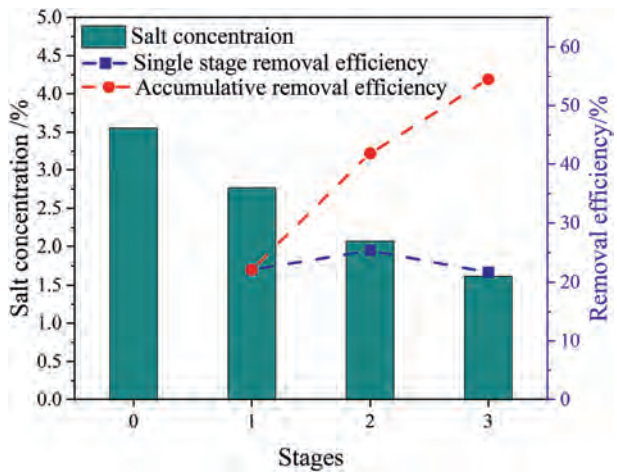

Fig. 11. The salt concentration and salt removal efficiency in three-stage desalination process with initial NaCl concentration of 3.5%.

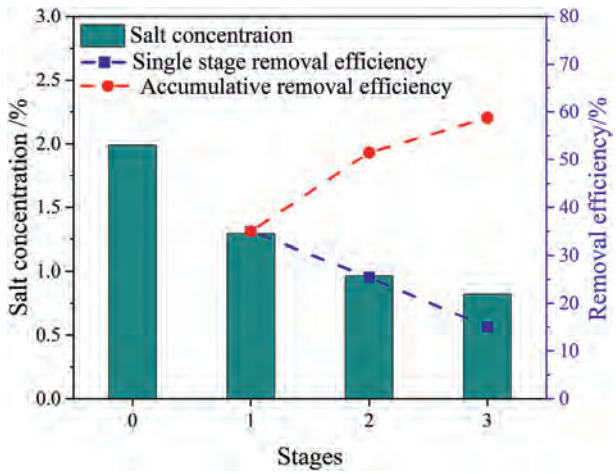

Fig. 12. The salt concentration and salt removal efficiency in three-stage desalination process with initial NaCl concentration of 2.0%.

of hydrates dissociated water. The pressure-driven filtration method can be used to strengthen the separation process of solid hydrate, residual unreacted gas and concentrated brine. Meanwhile, it is still need to optimize desalination stages, operation conditions and reactor to meet the water standard.

4. Conclusions

How to efficiently separate the hydrate phase and residual unreacted saltwater is one of the challenges for HBD. A pressure-driven filtration method was proposed in this work, which is simple and high-efficiently to separate the solid hydrate phase and residual concentrated saltwater. Based on this method, the salt removal efficiency of HBD was systematically studied. The experimental results show that when the extrusion pressure is higher than 5 MPa, the salt removal efficiency tends to stabilize, indicating that the solid gas hydrate and residual brine are maximally separated. When forming CO_2 hydrate from saltwater, the water conversion rate for single stage is around 20.39% to 43.01%, the corresponding highest salt removal efficiency is 52.54%, and the lowest desalination efficiency is 20.75%. The increase of water conversion rate will lead to the decrease of salt removal efficiency for HBD. When the initial salt concentration ranges from 0.3% to

8.0%, the salt removal efficiency of NaCl is 15.9% to 29.8%, while the salt removal efficiency of $CaCl_2$ is 28.9% to 45.5%, indicating the removal efficiency of solute $CaCl_2$ is higher than that of solute NaCl. The water recovery rate and salt removal efficiency for forming CO_2 hydrate is higher than that of forming methane hydrate. A large-scale experimental apparatus was developed to study the salt removal efficiency of multi-stage HBD. The NaCl concentration can decrease from 3.5% to 1.6% in three-stage hydrate desalination process, with a total salt removal efficiency of 54.48%. The NaCl concentration can further decrease from 2.0% to 0.8% in three-stage hydrate desalination process, with a total salt removal efficiency of 58.76%. It proves that the pressure-driven filtration is an effective method for separating to solid hydrate phase and residual unreacted saltwater phase to the most extent. The salt removal efficiency can be improved through adding the desalination stages.

CRediT Authorship Contribution Statement

Yiwei Wu: Writing − original draft, Methodology, Investigation, Formal analysis, Conceptualization. Zhenbin Xu: Methodology, Investigation, Formal analysis, Conceptualization. Xiaohui Wang: Writing− review & editing, Supervision, Conceptualization. Jin Cai: Investigation. Tenghua Zhang: Investigation. Peng Xiao: Investigation. Changyu Sun: Supervision, Conceptualization. Guangjin Chen: Supervision, Conceptualization.

Declaration of Competing Interest

The authors declare that they have no known competing financial interests or personal relationships that could have appeared to influence the work reported in this paper.

Acknowledgements

The financial support from the National Natural Science Foundation of China (22127812, 22278433, 22178379) and the National Key Research and Development Program of China (2021YFC2800902) are gratefully acknowledged.

References

[1] J.N. Zheng, M.J. Yang, Experimental investigation on novel desalination system *via* gas hydrate, *Desalination* 478 (2020) 114284.
[2] B.Y. Qiu, P. Gorgojo, X.L. Fan, Adsorption desalination: advances in porous adsorbents, *Chin. J. Chem. Eng.* 42 (2022) 151−169.
[3] M. Elimelech, W.A. Phillip, The future of seawater desalination: energy, technology, and the environment, *Science* 333 (6043) (2011) 712−717.
[4] Z.R. Chong, T.B. He, P. Babu, J.N. Zheng, P. Linga, Economic evaluation of energy efficient hydrate based desalination utilizing cold energy from liquefied natural gas (LNG), *Desalination* 463 (2019) 69−80.
[5] S.M.J. Seyed Sabour, B. Ghorashi, A comprehensive review of major water desalination techniques and mineral extraction from saline water, *Sep. Purif. Technol.* 349 (2024) 127913.
[6] S. Khodadousti, G. Kolliopoulos, Batteries in desalination: a review of emerging electrochemical desalination technologies, *Desalination* 573 (2024) 117202.
[7] H. Saleem, N. Abounahia, H.R. Siddiqui, S.J. Zaidi, Qatar desalination research: an overview, *Desalination* 564 (2023) 116802.
[8] P.G. Kumar, N. Thangapandian, V.S. Vigneswaran, P. Sundaram, A. Sathishkumar, S.C. Kim, R. Prabakaran, Energy, exergy, economic and environmental evaluation of solar desalination system comprising different enhanced surface absorber plates, *Desalination* 565 (2023) 116842.
[9] E.A. Grubert, A.S. Stillwell, M.E. Webber, Where does solar-aided seawater desalination make sense? A method for identifying sustainable sites, *Desalination* 339 (2014) 10−17.
[10] X. Zhang, X.Y. Zhang, L. Ma, B. Xu, H.B. Cong, Tailoring anionic solar evaporator with an enhanced donnan effect for a highly effective salt resistance desalination and water purification, *Sep. Purif. Technol.* 353 (2025) 128325.
[11] T.S. Chung, D.L. Zhao, J. Gao, K.J. Lu, C.F. Wan, M. Weber, C. Maletzko, Emerging R&D on membranes and systems for water reuse and desalination, *Chin. J. Chem. Eng.* 27 (7) (2019) 1578−1585.
[12] Y.Y. Wan, L.L. Yao, P. Cui, Graphene quantum dots doped poly(vinyl alcohol) hybrid membranes for desalination *via* pervaporation, *Chin. J. Chem. Eng.* 63 (2023) 226−234.
[13] H. You, W.C. Luo, P. Chammingkwan, T. Taniike, Achieving a balance between permeability and selectivity in a ZIF-8-matrix nanocomposite membrane for desalination, *Sep. Purif. Technol.* 351 (2024) 128126.
[14] J. Wang, J.H. Dai, Z.S. Jiang, B.L. Chu, F.M. Chen, Recent progress and prospect of flow-electrode electrochemical desalination system, *Desalination* 504 (2021) 114964.
[15] X.N. Liu, B.H. Zhao, Y.Y. Hu, L.Y. Huang, J.X. Ma, S.Q. Xu, Z.L. Xia, X.Y. Ma, S.C. Ma, Enhancing capacitive deionization performance and cyclic stability of nitrogen-doped activated carbon by the electro-oxidation of anode materials, *Chin. J. Chem. Eng.* 69 (2024) 23−33.
[16] H.Y. Wang, H.Y. Gang, D. Wei, Y.J. He, S. Issaka Alhassan, L.J. Yan, B.C. Wu, Y.Y. Cao, L.F. Jin, L. Huang, Bismuth−titanium alloy nanoparticle@porous carbon composite as efficient and stable Cl-storage electrode for electrochemical desalination, *Sep. Purif. Technol.* 296 (2022) 121375.
[17] J.X. Sun, Y. Wang, S.C. Xu, S.C. Wang, Energy recovery device with a fluid switcher for seawater reverse osmosis system, *Chin. J. Chem. Eng.* 16 (2) (2008) 329−332.
[18] A.Y. Goren, Y.A. Jarma, N. Kabay, , B.B. A., H.E. Okten, Boron removal from geothermal brine using hybrid reverse Osmosis/Microbial desalination cell system, *Sep. Purif. Technol.* 309 (2023) 123006.
[19] H. Abulkhair, S. Nallakukkala, M.S. Khan, I.A. Moujdin, E. Almatrafi, O. Bamaga, A. Alsaiari, M.H. Albeirutty, B. Lal, A. Mohd Shariff, Desalination of produced water *via* carbon dioxide hydrate using filter-based hydrate desalination reactor, *Sep. Purif. Technol.* 332 (2024) 125849.
[20] S.C. Sun, Y.P. Zhao, L.L. Gu, J.H. Cui, L.T. Sun, S.T. Meng, Energy analysis of a flue gas hydrate-based desalination system with liquefied natural gas cold energy, *Nat. Gas. Ind. B* 10 (6) (2023) 613−625.
[21] J.B. Zhang, X.L. Xing, Z.Y. Yin, N. Mao, T.B. He, Evaluating CO_2+C_3H_8 hydrate kinetics with cyclopentane and graphite for sustainable hydrate-based desalination, *J. Clean. Prod.* 384 (2023) 135365.
[22] J.N. Zheng, F.B. Cheng, Y.P. Li, L. Xin, M.J. Yang, Progress and trends in hydrate based desalination (HBD) technology: a review, *Chin. J. Chem. Eng.* 27 (9) (2019) 2037−2043.
[23] A. Parker, Potable water from sea-water, *Nature* 149 (1942) 184−186.
[24] G.R. Dickens, M.S. Quinby-Hunt, Methane hydrate stability in seawater, *Geophys. Res. Lett.* 21 (19) (1994) 2115−2118.
[25] Y.N. Lv, S.S. Wang, C.Y. Sun, J. Gong, G.J. Chen, Desalination by forming hydrate from brine in cyclopentane dispersion system, *Desalination* 413 (2017) 217−222.
[26] E.G. Hammerschmidt, Formation of gas hydrates in natural gas transmission lines, *Ind. Eng. Chem.* 26 (8) (1934) 851−855.
[27] R. Du, Y.X. Fu, L.X. Zhang, J.F. Zhao, Y.C. Song, Z. Ling, Desalination of high-salt brine *via* carbon materials promoted cyclopentane hydrate formation, *Desalination* 534 (2022) 115785.
[28] H. Fakharian, H. Ganji, A. Naderifar, Desalination of high salinity produced water using natural gas hydrate, *J. Taiwan Inst. Chem. Eng.* 72 (2017) 157−162.
[29] H.L. Sun, S. Wang, S.Q. Wang, Y.C. Song, Z. Ling, L.X. Zhang, Rapid processing of dispersed hydrate-based purification for high-yield seawater desalination and wastewater treatment, *Desalination* 604 (2025) 118741.
[30] Z. Ling, C.R. Shi, F. Li, Y.X. Fu, J.F. Zhao, H.S. Dong, Y.M. Yang, H. Zhou, S. Wang, Y.C. Song, Desalination and Li^+ enrichment *via* formation of cyclopentane hydrate, *Sep. Purif. Technol.* 231 (2020) 115921.
[31] F.Y. Mi, Z.J. He, F.L. Ning, Molecular insight on CO_2/C_3H_8 mixed hydrate formation from the brine for sustainable hydrate-based desalination, *Sep. Purif. Technol.* 353 (2025) 128244.
[32] H. Abulkhair, S. Nallakukkala, I.A. Moujdin, E. Almatrafi, O. Bamaga, A. Alsaiari, M.H. Albeirutty, J.R.D. Nallakukkala, B. Lal, A.M. Shariff, Desalination of produced water *via* CO_2 + C_3H_8 hydrate formation, *Sep. Purif. Technol.* 315 (2023) 123711.
[33] J. Mok, M. Park, W. Choi, K.C. Kang, S. Lee, J.D. Lee, Y. Seo, Investigation of theoretical maximum water yield and efficiency-optimized temperature for cyclopentane hydrate-based desalination, *Water Res.* 246 (2023) 120707.
[34] M. Maniavi Falahieh, M. Bonyadi, A. Lashanizadegan, A new hybrid desalination method based on the CO_2 gas hydrate and capacitive deionization processes, *Desalination* 502 (2021) 114932.
[35] E.M. Salilih, M.N. Khan, O. Bamaga, I. Ahmed, M. Albeirutty, E. Almatrafi, H. Abulkhair, H. Alhumade, A. Bamasag, M.G.H. Haidar, Thermal analysis of integrated hydrate-based desalination system with intermediate fluid type LNG vaporizer, *J. Clean. Prod.* 420 (2023) 138405.
[36] K.N. Park, S.Y. Hong, J.W. Lee, K.C. Kang, Y.C. Lee, M.G. Ha, J.D. Lee, A new apparatus for seawater desalination by gas hydrate process and removal characteristics of dissolved minerals (Na^+, Mg^{2+}, Ca^{2+}, K^+, B^{3+}), *Desalination* 274 (1−3) (2011) 91−96.
[37] K.C. Kang, P. Linga, K.N. Park, S.J. Choi, J.D. Lee, Seawater desalination by gas hydrate process and removal characteristics of dissolved ions (Na^+, K^+, Mg^{2+}, Ca^{2+}, B^{3+}, Cl^-, SO_4^{2-}), *Desalination* 353 (2014) 84−90.
[38] J. Chen, J.J. Wu, J.F. Xu, Q. Yuan, B. Deng, C.Z. Chen, Z. Li, Experiments and insights of desalination by a freezing/thawing method at low subcooling, *Chin. J. Chem. Eng.* 28 (12) (2020) 3011−3017.
[39] S.M. Montazeri, N. Kalogerakis, G. Kolliopoulos, CO_2 nanobubbles as a novel kinetic promoter in hydrate-based desalination, *Desalination* 574 (2024) 117296.

[40] H.S. Truong-Lam, S.D. Seo, C. Jeon, G.P. Lee, J.D. Lee, A gas hydrate process for high-salinity water and wastewater purification, *Desalination* 529 (2022) 115651.
[41] P. Babu, A. Nambiar, Z.R. Chong, N. Daraboina, M. Albeirutty, O.A. Bamaga, P. Linga, Hydrate-based desalination (HyDesal) process employing a novel prototype design, *Chem. Eng. Sci.* 218 (2020) 115563.
[42] S. Han, J.Y. Shin, Y.W. Rhee, S.P. Kang, Enhanced efficiency of salt removal from brine for cyclopentane hydrates by washing, centrifuging, and sweating, *Desalination* 354 (2014) 17–22.
[43] X.H. Wang, X.J. Xu, J. Cai, Y.W. Wu, Y.X. Chen, W.X. Pang, C.Y. Sun, G.J. Chen, Experimental study on the intrinsic dissociation rate of methane hydrate, *Chem. Eng. Sci.* 282 (2023) 119278.
[44] X.H. Wang, X.J. Xu, J. Cai, H.X. Zheng, Y.X. Chen, W.X. Pang, Y. Yu, C.Y. Sun, G.J. Chen, CO_2 concentration in aqueous solution from gas–liquid equilibrium system to gas–liquid–hydrate coexistence system, *Gas Sci. Eng.* 115 (2023) 205024.
[45] C.G. Xu, X.S. Li, K.F. Yan, X.K. Ruan, Z.Y. Chen, Z.M. Xia, Research progress in hydrate-based technologies and processes in China: a review, *Chin. J. Chem. Eng.* 27 (2019) 1998–2013.
[46] E.P. Brown, S.J. Hu, J. Wells, X.H. Wang, C.A. Koh, Direct measurements of contact angles on cyclopentane hydrates, *Energy Fuel.* 32 (6) (2018) 6619–6626.
[47] F. Thomas, D. Dalmazzone, J.F. Morris, Contact angle measurements on cyclopentane hydrates, *Chem. Eng. Sci.* 229 (2021) 116022.
[48] F. Asadi, M. Ejtemaei, G. Birkett, D.J. Searles, A.V. Nguyen, The link between the kinetics of gas hydrate formation and surface ion distribution in the low salt concentration regime, *Fuel* 240 (2019) 309–316.
[49] N.N. Nguyen, A.V. Nguyen, The dual effect of sodium halides on the formation of methane gas hydrate, *Fuel* 156 (2015) 87–95.
[50] F. Farhang, A.V. Nguyen, M.A. Hampton, Influence of sodium halides on the kinetics of CO_2 hydrate formation, *Energy Fuel.* 28 (2) (2014) 1220–1229.
[51] D.F. Liu, G. Ma, L.M. Levering, H.C. Allen, Vibrational spectroscopy of aqueous sodium halide solutions and air–liquid interfaces: observation of increased interfacial depth, *J. Phys. Chem. B* 108 (7) (2004) 2252–2260.
[52] X.H. Wang, Y.F. Wang, Y. Xie, C.Y. Sun, G.J. Chen, Study on the decomposition conditions of gas hydrate in quartz sand–brine mixture systems, *J. Chem. Thermodyn.* 131 (2019) 247–253.
[53] W. Ke, D.Y. Chen, A short review on natural gas hydrate, kinetic hydrate inhibitors and inhibitor synergists, *Chin. J. Chem. Eng.* 27 (9) (2019) 2049–2061.
[54] M. Kishimoto, S. Iijima, R. Ohmura, Crystal growth of clathrate hydrate at the interface between seawater and hydrophobic-guest liquid: effect of elevated salt concentration, *Ind. Eng. Chem. Res.* 51 (14) (2012) 5224–5229.
[55] Y.J. Zhu, Y.Z. Chen, Y. Xie, J.R. Zhong, X.H. Wang, P. Xiao, Y.F. Sun, C.Y. Sun, G.J. Chen, Microscopic experimental study on the effects of NaCl concentration on the self-preservation effect of methane hydrates under 268.15 K, *Chin. J. Chem. Eng.* 73 (2024) 1–14.
[56] M.M. Falahieh, M. Bonyadi, A. Lashanizadegan, Effect of different salts on the kinetic parameters of the carbon dioxide hydrate formation, *J. Nat. Gas Sci. Eng.* 100 (2022) 104461.
[57] B. Sowa, X.H. Zhang, P.G. Hartley, D.E. Dunstan, K.A. Kozielski, N. Maeda, Formation of ice, tetrahydrofuran hydrate, and methane/propane mixed gas hydrates in strong monovalent salt solutions, *Energy Fuel.* 28 (11) (2014) 6877–6888.
[58] B. Sowa, X.H. Zhang, K.A. Kozielski, P.G. Hartley, D.E. Dunstan, N. Maeda, Nucleation probability distributions of methane–propane mixed gas hydrates in salt solutions and urea, *Energy Fuel.* 29 (10) (2015) 6259–6270.
[59] J.J. Zheng, N.K. Loganathan, P. Linga, Natural gas storage *via* clathrate hydrate formation: effect of carbon dioxide and experimental conditions, *Energy Proc.* 158 (2019) 5535–5540.
[60] F. Golkhou, A. Haghtalab, Measurement and thermodynamic modeling of carbon dioxide hydrate formation conditions using dry water through hydrophobic nano silica, *J. Nat. Gas Sci. Eng.* 68 (2019) 102906.